JACS
JOURNAL OF THE AMERICAN CHEMICAL SOCIETY
Article
pubs.acs.org/JACS

Facile Route to Quadruply Annulated Borepins

Kai Schickedanz, Julian Radtke, Michael Bolte, Hans-Wolfram Lerner, and Matthias Wagner*

Institut für Anorganische und Analytische Chemie, Goethe-Universität Frankfurt, Max-von-Laue-Strasse 7, D-60438 Frankfurt (Main), Germany

Supporting Information

ABSTRACT: A two-step synthesis sequence furnishes quadruply annulated borepins in high yields. The first step involves a nucleophilic substitution reaction between aryl−BF_3K salts (aryl = mesityl, phenyl) and lithiated bromonapthalene derivatives $LiNaph^{Br,R}$ ($HNaph^{Br,R}$ = 8-bromonaphthalene (a), 5-bromoacenaphthene (b), 5-bromoacenaphthylene (c)). In the second step, the resulting heteroleptic triarylboranes aryl−$B(Naph^{Br,R})_2$ (**3a−c**) are subjected to an intramolecular Ni-mediated Yamamoto reaction to close the seven-membered rings and create the borepins **4a−c**. Only in the case of **3b** is the Yamamoto reaction accompanied by a C−H activation reaction furnishing the 7-hydro-7-borabenzo[*de*]anthracene derivative **5**. The product ratio **4b**/**5** can be influenced by control of the local Ni(0) concentration. The borepins **4a−c** are benchtop stable and highly soluble even in hexane. Compounds **4a−c** undergo reversible one-electron reduction; **4c** is also able to accept a second electron in a reversible manner and already at moderate potential values ($E_{1/2}$ = −1.49 V and −1.84 V (vs FcH/FcH^+)). **4a**, **4b**, and **5** show photoluminescence in the blue-green region of the spectrum, while **4c** is nonfluorescent, which is likely attributable to an intramolecular charge-transfer transition.

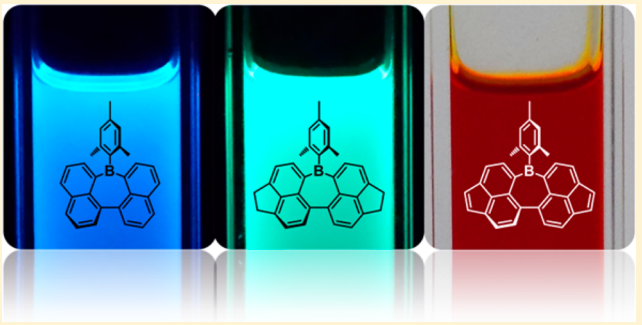

I. INTRODUCTION

Research on unsaturated boron-containing ring compounds has intrigued chemists for decades. Because of its vacant p orbital, the boron atom acts as an electronically perturbative element on the cyclic π-electron system.[1−5] Boron incorporation is thus a powerful tool to further develop and evaluate fundamental theories of chemical bonding, in particular, the concept of aromaticity.

The formal insertion of BH fragments into cyclobutadiene and benzene as the prototypical antiaromatic and aromatic molecules leads to boroles[6] on the one hand and borepins[7] on the other (Chart 1). While the pristine borole, as well as its mesityl-protected derivative, have so far eluded synthesis (only computed data are known[8]), experimental NMR shift values of the parent BH borepin are published and 1-mesitylborepin is even stable in air for short periods of time.[9,10] Thus, characteristic reactivity patterns of the parent all-carbon compounds are still reflected in the behavior of their ring-expanded boron congeners. By the same token, 1,4-dihydro-1,4-diborabenzene, the product of a 2-fold BH insertion into cyclobutadiene, does not exist as a planar, D_{2h} symmetric molecule, but only in the form of a pentagonal−pyramidal carborane cluster;[11−13] 1,4-dimesityl-1,4-dihydro-1,4-diborabenzene is entirely unknown.

Chart 1. Structures of Cyclobutadiene and Benzene and Their Products after Formal BH Insertion

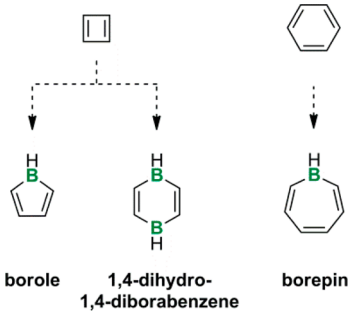

A thorough investigation of electronic structure−property relationships is best carried out on the unsubstituted, pristine heterocycles. However, when it comes to practical applications of these compounds, e.g., as homogeneous catalysts[14−16] or opto-electronic materials,[4,17,18] chemical stability becomes a key issue.

As has been documented on multiple occasions, benzannulation provides an efficient means of generating more inert derivatives. Indeed, the doubly benzene-fused borole (9-borafluorene)[19,20] and the corresponding 1,4-dihydro-1,4-diborabenzene (9,10-dihydro-9,10-diboraanthracene)[21,22] are synthetically accessible, even though the former still possesses a strong tendency to undergo ring-opening reactions.[23−25] In addition to the stabilizing effect, benzannulation increases the delocalized π-electron systems of the molecules, which often brings about improved redox activities and pronounced photoluminescence.[26]

In addition, the dibenzo(*b*,*f*) derivative **DBB** (Chart 2) of the formally aromatic borepin possesses a chemically much more

Received: January 9, 2017
Published: January 26, 2017

DOI: 10.1021/jacs.7b00268
J. Am. Chem. Soc. 2017, 139, 2842−2851

Chart 2. Structures of Dibenzo- (DBB), Dithieno- (DTB), and Dinaphtho-Fused Borepins (DNB(*b,f*) and DNB(*bc,ef*))

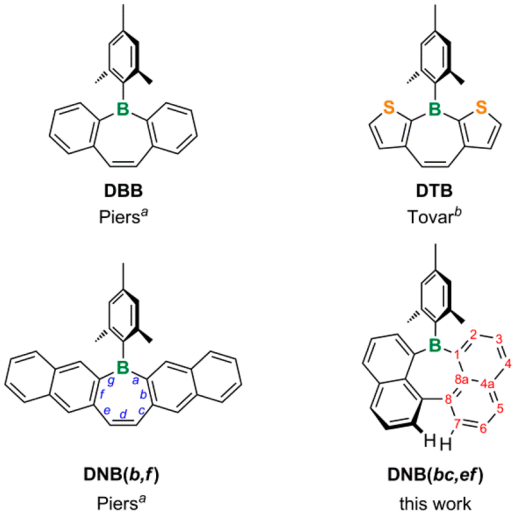

[a]Reference 27. [b]Reference 33

robust scaffold than the pristine heterocycle.[27] **DBB** undergoes a quasi-reversible redox transition at $E_{1/2}$ = −2.56 V (THF, vs FcH/FcH^+) and shows blue photoluminescence (λ_{em} = 400 nm, ϕ_{PL} = 70%). An anodic shift of the redox potential, accompanied by a bathochromic shift of the emission wavelengths, was achieved through linear annulation of one or two further benzene rings (cf. **DNB(*b,f*)**; Chart 2), albeit at the expense of a precipitous drop of the fluorescence quantum yields (ϕ_{PL} = 1%). As an alternative to benzannulation, dangling phenyl groups have been installed at the **DBB** core in the *meta* positions relative to the boron atom.[28] Tovar and co-workers have prepared a systematic series of doubly *meta*- or *para*-substituted **DBB**s, many of them through late-stage modification of corresponding halogenated **DBB**s.[29,30] In the *meta* isomers, charge delocalization should occur mainly through the stilbene fragment without participation of the boron center. Contrary to that, when functional groups are placed in the *para* positions, the boron atom becomes a more integral part of the conjugation pathway. Indeed, the installation of *meta* substituents was found to decrease the optical bandgap of the **DBB** system while *para* substitution raises its electron affinity.[30]

Recent progress regarding derivatization through annulation has provided access to *meta*- and *para*-*B*-entacenes (polycyclic aromatics containing two borepin rings)[29,31,32] and to doubly thiophene-fused borepins[33] (cf. **DTB**; Chart 2).[34] Herein, we report on the first examples of quadruply benzannulated borepins (**DNB(*bc,ef*)**; Chart 2), which have been obtained via a fundamentally new synthesis strategy and possess remarkable optoelectronic properties.

II. RESULTS AND DISCUSSION

Design Considerations. Extended planar polycyclic aromatic hydrocarbons (PAHs) often suffer from poor solubilities, which limit the options for liquid-phase characterization and processability. One way to tackle this problem is to introduce solubilizing side chains. As a downside of this approach, proper π-stacking of the molecules in the emission/electron-transport layers of potential devices can be negatively affected. To circumvent this disadvantage, we recently proposed inducing moderate distortions of the PAH framework and, in a proof-of-principle project, prepared a highly soluble boron-doped [4]helicene.[35] Herein, we now apply related design guidelines to the development of **4a–c** (Scheme 1): The annulation of four benzene moieties to the borepin ring is intended to increase the π-electron system and thus modify the optoelectronic properties of the pristine compound. The distribution of the benzene rings around the heterocycle creates a sterically congested, distorted bay region.

Synthesis of Quadruply Annulated Borepins. The best-established synthesis approach to (functionalized) **DBB**s first generates a *Z*-olefin bridge between two brominated aryl rings by means of a Wittig reaction (Scheme 1).[27,29,30,36] Subsequent lithium–bromine exchange, followed by the addition of Me_2SnCl_2, furnishes the corresponding stannepins. Boron incorporation is achieved at the final stage of the reaction sequence through tin–boron exchange using BCl_3. Protection of the boron centers by mesityl (Mes) substituents results in moderately air- and moisture-stable derivatives; the synthesis of long-term stable **DBB**s, which are also sufficiently inert for further functionalization via Kumada- or Suzuki-coupling

Scheme 1. Synthesis of (*b,f*)-Annulated DBB[a] (A) and Synthesis of the (*bc,ef*)-Annulated Borepin Derivatives 4a–c (B)

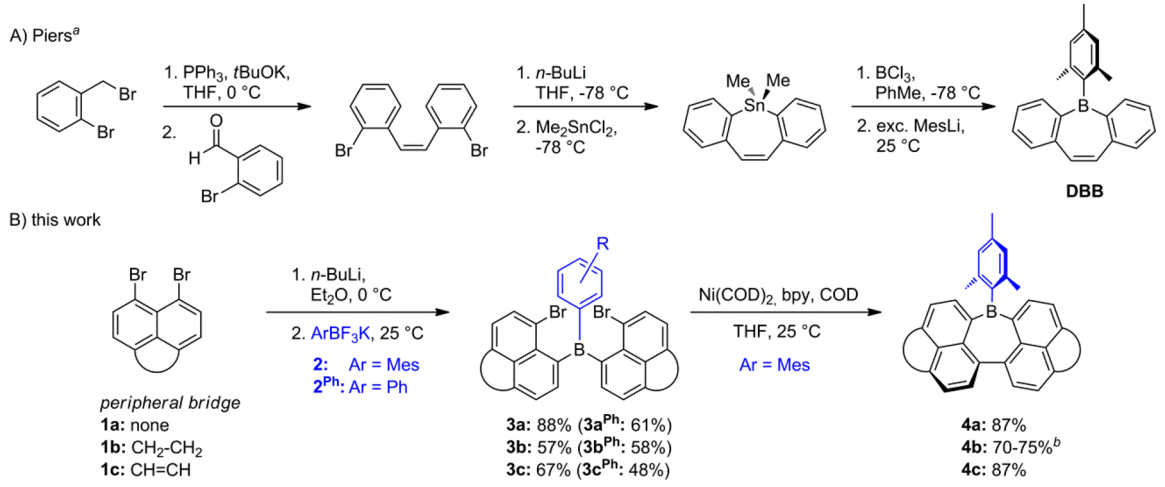

[a]Reference 27. [b]Combined yield of **4b** and **5** (cf. Scheme 3); the product ratio is strongly dependent on the reaction conditions.

DOI: 10.1021/jacs.7b00268
J. Am. Chem. Soc. 2017, 139, 2842–2851

protocols, requires the introduction of a sterically even more demanding Mes* group (Mes* = 2,4,6-tri-*tert*-butylpenyl).[29] Direct quenching of the dilithiated intermediate with Mes−$B(OMe)_2$ would not only be more step-economic but also avoid the use of toxic organotin reagents and corrosive boron halides. So far, however, this shortcut was only viable in special cases when dimetalated (*Z*)-thienyl(aryl)ethenes were employed.[33]

The three-step borepin synthesis strategy developed by us is based on boron-containing precursors and closes the seven-membered ring in the last step by forming the C−C bond at the *d* position (Scheme 1; Chart 2): First, an aryl boronic acid is converted into the potassium trifluoroborate salt **2** by means of KHF_2.[37] Second, the air- and moisture-stable triarylboranes **3a−c** are prepared from **2** and an equimolar mixture of *n*-BuLi with the dibromonaphthalene derivatives **1a−c**.

Third, an intramolecular, Ni-mediated Yamamoto-type reaction is applied for the reductive C−C coupling between the pendant naphthyl moieties to form the desired borepins **4a−c**.

Some further comments regarding details of the individual synthesis steps are in order:

Step 1: Plenty of benchtop-stable organotrifluoroborates are readily available, e.g., through the work of Genet and Molander.[38] We thus have the opportunity to choose our key starting materials from a broad variety of compounds, which renders our synthesis approach highly modular. We already benefitted from this modularity because it enabled us to effortlessly synthesize the phenyl congeners $\mathbf{3a}^{Ph}$−$\mathbf{3c}^{Ph}$ of the mesityl boranes, which later on proved to be useful to gain important structural information about the borepin precursors (see below).

Step 2: At a first glance, the formal nucleophilic substitution reaction between a negatively charged trifluoroborate (**2**) and a naphthyl anion may seem counterintuitive,[39] and related examples are indeed rare.[35,40−43] However, we reproducibly obtained high yields of **3a** (88%), **3b** (57%), and **3c** (67%), while none of our attempts to replace **2** by Mes−BR_2 (R = OMe, Br) was met with success. In addition, the reaction between Mes−BBr_2 and 1-bromo-8-(trimethylstannyl)naphthalene did not provide useful quantities of **3a**. In conclusion, even though aryltrifluoroborates are still mainly used for Pd-catalyzed cross-coupling reactions, they can obviously also serve as versatile starting materials for the synthesis of heteroleptic triarylboranes, even in those cases where common aryl boronate esters or aryl boron dihalides fail to give the desired products.

Step 3: Ni complexes are well-known catalysts for the homocoupling of aryl halides to give biaryls.[44] Using **3a** as the prototypical system, we specifically tested protocols introduced by Iyoda,[45] Colon,[46] and Percec[47] (Scheme 2). After workup to remove (paramagnetic) Ni species, ^{1}H NMR spectroscopy revealed in all cases that the starting material **3a** still constituted by far the major component of the crude reaction mixtures (see the SI for plots of the spectra). Importantly, a number of additional minor resonances indicated at least some conversion and therefore pointed toward an initially active catalyst system. To confirm this conclusion, a number of further experiments were carried out (based on Colon's approach): First, and contrary to the previous experiments, we preformed the active catalyst, which indeed showed the typical red-brown color in DMF solution. After the addition of **3a**, the color slowly faded while the solution was heated at 75 °C overnight. The outcome, however, remained the same as in the previous experiments (NMR spectroscopic control). Second, we repeated the last

Scheme 2. Synthesis of 4a and 4c Starting from 3a and 3c[a]

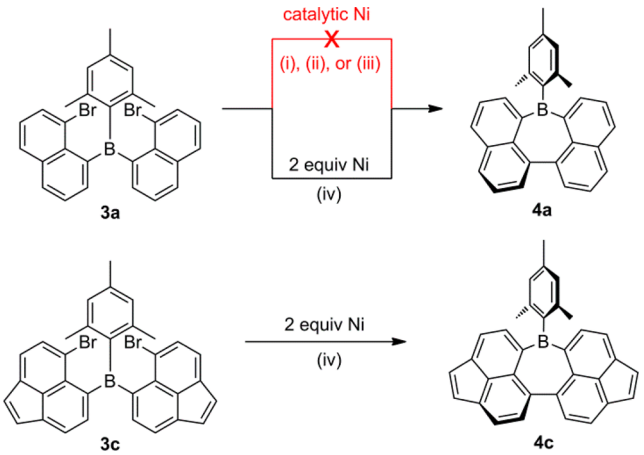

[a]Reaction conditions: (i) Iyoda: $NiBr_2(PPh_3)_2$, Et_4NI, PPh_3, exc Zn, THF, 65 °C, 24 h; (ii) Colon: $NiCl_2$, PPh_3, exc Zn, NaBr or bpy, DMF, 75 °C, 24 h; (iii) Percec: $NiCl_2(PPh_3)_2$, Et_4NI, exc Zn, THF, 65 °C, 24 h; (iv) $Ni(COD)_2$ (2.0 equiv), bpy, COD, THF, 25 °C, overnight.

experiment but added some bromobenzene after 15 h. As expected, we again did not observe borepin formation, but the bromobenzene was fully consumed and biphenyl was obtained (according to thin-layer chromatography and NMR spectroscopy).

We therefore conclude that the aimed-for C−C coupling reaction on **3a** cannot be performed in a fashion that is catalytic in the Ni complex. A possible explanation is offered by the intramolecular nature of the process: Numerous different proposals for the mechanism of Ni-catalyzed homocouplings are still under discussion.[44] In particular, the question whether the reaction involves mono- or dinuclear Ni complexes has not finally been answered. Given the low catalyst loading, it is statistically unlikely for the same molecule **3a** to insert two Ni atoms into both of its C−Br bonds. As a result, intramolecular C−C coupling will hardly take place if a dinuclear mechanism is operative or if the reaction requires metathesis between two Ni intermediates (this is in stark contrast to intermolecular reactions because two active Ni−aryl complexes can approach each other by diffusion).

To test this hypothesis, the Colon protocol was next carried out on **3a** in a stoichiometric fashion, which this time resulted in the quantitative consumption of the starting material, however, without furnishing appreciable quantities of **4a**. This immediately raised the question whether **4a** is not generated in the first place or whether it is not compatible with the forcing conditions required for the Colon coupling (i.e., elevated temperatures, strong donor solvent DMF, strongly reducing Zn powder with a large reactive surface area). We therefore heated a DMF solution of authentic **4a** in the presence of $NiCl_2$, PPh_3, exc Zn, and bpy at 75 °C overnight (bpy = 2,2′-bipyridyl). No degradation was observed.

Taken together, these results lead to the conclusion that the most common Ni-catalyzed C−C coupling methods are not applicable for the synthesis of the borepins **4a−c**, even if the metal salts are employed in stoichiometric quantities. We therefore turned next to Yamamoto-type protocols[48] and stoichiometric mixtures of $Ni(COD)_2$/bpy/COD as the coupling reagent (COD = 1,5-cyclooctadiene). For reasons of simplicity, we will nevertheless refer to this mixture as "the catalyst system" even

DOI: 10.1021/jacs.7b00268
J. Am. Chem. Soc. 2017, 139, 2842−2851

though we are aware of the fact that only part of the Ni ions are catalytically active whereas most of the $Ni(COD)_2$ likely replaces Zn as a stoichiometric reducing agent. Under Yamamoto conditions, the common reactivities of C−Cl and C−Br bonds toward Ni complexes[49] are inverted such that aryl bromides become the more suitable starting materials.[48] Moreover, we have already applied an intramolecular Yamamoto reaction successfully to the synthesis of a boron-doped [4]helicene.[35] Indeed, the reaction of 2 equiv of the catalyst system with **3a** or **3c** in THF afforded both borepins **4a** and **4c** in excellent yields of 87% (Scheme 2). The acenaphthene derivative **3b** is a special case because borepin formation is accompanied by a C−H activation reaction furnishing compound **5**, which contains a six-membered boracycle (Scheme 3).

Scheme 3. Synthesis of 4b and 5, Starting from 3b[a]

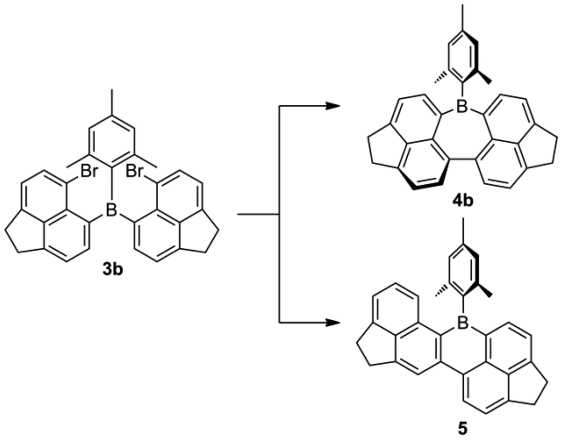

product ratio

	A	B	C
4b : **5**	3 : 1	1 : 1	1 : 2.5

[a]Reaction conditions: (A) dropwise addition of **3b** to the preformed catalyst system in THF, 35 °C; (B) addition of $Ni(COD)_2$ in one portion to a solution of **3b**, bpy, and COD in THF, 30 °C; (C) dropwise addition of the preformed catalyst system to a solution of **3b** in THF, 25 °C.

The combined yields of **4b** and **5** constantly ranged between 70 and 75%, but the ratio **4b**/**5** was heavily dependent on the reaction conditions. If the focus lies on the borepin **4b**, the precursor **3b** should be added to the preformed catalyst system at 35 °C in THF. If the yield of the C−H activation product **5** is to be maximized, the reaction should be carried out at room temperature by dropwise addition of the preformed catalyst system in THF to a dilute solution of **3b** in the same solvent (see below for more detailed mechanistic considerations to rationalize these observations).

Different from the borepins reported by Piers[27] and Tovar,[29,30] our mesityl-substituted derivatives **4a**−**c** are long-term stable at ambient conditions: NMR spectroscopic monitoring of solutions of **4a** in $CDCl_3$, to which water had deliberately been added, showed no sign of borepin decomposition over a period of 1 month. However, a switch from the mesityl- to the phenyl-protected borepins $\mathbf{4a^{Ph}}$−$\mathbf{4c^{Ph}}$ is not tolerated. We prepared the corresponding compounds starting from $\mathbf{3a^{Ph}}$−$\mathbf{3c^{Ph}}$ but found them to undergo partial protonolysis with cleavage of the exocyclic B−Ph bonds upon methanolic workup. The resulting hydroxy borepins have been identified NMR spectroscopically as the major constituents of the crude product mixtures. However, since this publication is devoted to air- and moisture-stable borepins, we have put the focus of all further investigations on the mesityl derivatives **4a**−**c**.

NMR Spectroscopic Characterization of the Precursor Molecules 3a−c and the Borepins 4a−c. Upon conversion of Mes−BF_3K to **3a**−**c**, the ^{11}B NMR signal of the starting material (4 ppm, q, $^1J_{BF}$ = 58 Hz) vanishes and broad resonances in the range between 65 and 70 ppm appear instead. In contrast, the further transformation of **3a**−**c** to the borepin derivatives **4a**−**c** has only a negligible influence on the ^{11}B NMR spectra. The respective resonance of **5**, in which the boron atom is part of a six- rather than a seven-membered ring, appears significantly upfield-shifted at 59 ppm. All of these values are typical for three-coordinate triarylboranes.[50]

Each of the precursor molecules **3a**−**c** gives rise to two sets of signals in the ^1H as well as the ^{13}C NMR spectrum. This is in accordance with the presence of C_1- and C_2-symmetric rotamers, which do not interconvert on the NMR time scale (see below for results of variable-temperature NMR experiments and X-ray crystal-structure analyses). A similar phenomenon has previously been observed for other bis(8-bromonaphth-1-yl)boranes.[35,51] Due to the lack of symmetry, each of the C_1 rotamers gives two resonances for the mesityl *o*-CH_3 and another two for the *m*-CH protons, while the *p*-CH_3 group leads to only one signal. In the corresponding C_2 rotamers, the mesityl *o*-CH_3 substituents (and also the *m*-CH protons) are magnetically equivalent. We have used the integral values of these resonances to determine the relative proportions of the rotamer pairs C_1:C_2 as 1:3 (**3a**), 2.5:1 (**3b**), and 3.3:1 (**3c**). The resonance sets belonging to C_1-**3b** and C_1-**3c** have been fully assigned. This was not possible in the case of C_1-**3a** due to low signal intensities and considerable signal overlaps. Some characteristic features became obvious upon a closer inspection of the NMR data of **3b** and **3c**: The resonances of the protons in the positions *ortho* and *meta* to the bromine substituents have very similar chemical shift values in C_1/C_2-**3b** or C_1/C_2-**3c**. This is no longer true for the signals of the protons *meta* to the respective boron atom, and especially the *ortho* resonances show an extremely large spread (cf. C_1/C_2-**3b**: 6.54, 7.37/7.98 ppm; C_1/C_2-**3c**: 6.63, 7.47/8.01 ppm; in the ^{13}C NMR spectra, signals belonging to related carbon atoms are generally clustered closely together). These observed chemical shift differences are likely caused by magnetic anisotropy effects resulting from the aromatic ring currents. Differences in the chemical environments between the individual rotamers are obviously more pronounced for protons belonging to the boron-bonded rings than for protons belonging to the peripheral, bromine-bonded rings.

Upon going from the triarylboranes **3a**−**c** to the borepins **4a**−**c**, the carbon atoms C8 involved in the C−C coupling reaction experience a characteristic downfield shift from 117.9−125.1 ppm to 137.0−141.5 ppm. Moreover, the protons H7 are now pointing into a newly formed bay region (Chart 2). In planar polycyclic aromatic hydrocarbons (PAHs), such hydrogen atoms are typically strongly deshielded.[52] In the ^1H NMR spectra of **4a**−**c** the corresponding H7 resonances appear at 7.44, 7.62, and 7.90 ppm, respectively. This observed trend indicates **4a** to feature the most twisted molecular scaffold within the series and, in turn, the largest distance between the two H7 atoms (Table 1).

Structural Peculiarities of $\mathbf{3a^{Ph}}$−$\mathbf{3c^{Ph}}$, 3a−c, and 4a−c. According to room-temperature NMR spectroscopy, the precursor

DOI: 10.1021/jacs.7b00268
J. Am. Chem. Soc. 2017, 139, 2842−2851

Table 1. Three Different Views of the Crystallographically Determined Molecular Structure of 4a (Top, H Atoms are Omitted for Clarity) and the Computed Structures of 4a–c (Bottom)

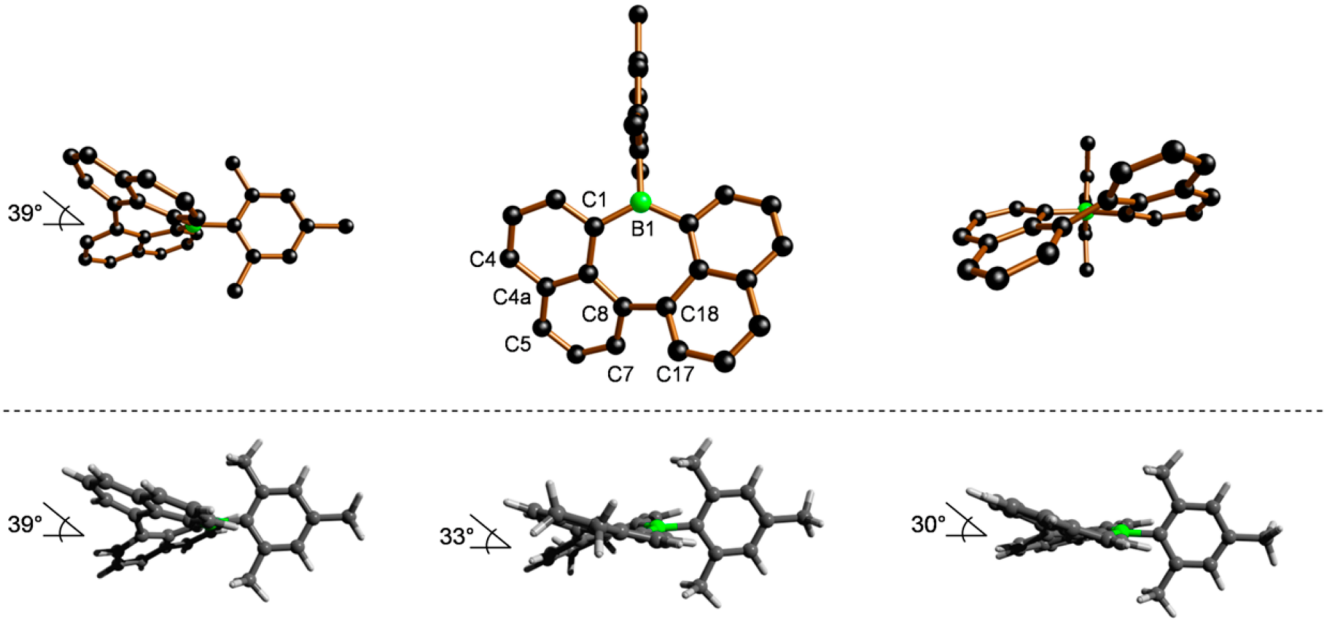

	4a (X-ray)	4a[a] (calc)	4b[a] (calc)	4c[a] (calc)	DBB[b] (X-ray)
B–C (endo)[c]	1.563(2) Å	1.564 Å	1.561 Å	1.563 Å	1.564 Å
B–C (exo)	1.595(2) Å	1.595 Å	1.596 Å	1.594 Å	1.586 Å
C–C (#d)	1.502(2) Å	1.497 Å	1.492 Å	1.487 Å	1.342 Å
C–B–C (endo)	127.3(1)°	127.2°	126.2°	125.8°	125.2°
C–B–C (exo)[c]	116.4(1)°	116.4°	116.9°	117.1°	117.4°
C4–C4a–C5[c]	119.8(2)°	119.2°	111.0°	108.5°	
C7–C8–C18–C17	38.9(2)°	39.2°	32.8°	30.4°	

[a]B3LYP/6-31G* level of theory. [b]Reference 27. [c]Average values.

molecules **3b** and **3c** preferentially adopt a C_1-symmetric conformation, whereas the C_2 rotamer is thermodynamically favored for the naphthyl derivative **3a**. The three phenyl congeners $\mathbf{3a}^{Ph}$–$\mathbf{3c}^{Ph}$ also prefer the C_2-symmetric form: At −30 °C, their bromine-carrying substituents are magnetically equivalent and their proton resonances are well resolved. Upon heating, the signals broaden and coalesce at about 0 °C. A fully resolved ^{1}H NMR spectrum is again obtained at approximately 60 °C. This indicates that the C_2 rotamers are first frozen on the NMR time scale, yet free rotation about the B–C bonds of $\mathbf{3a}^{Ph}$–$\mathbf{3c}^{Ph}$ takes place already at temperatures at which the mesityl derivatives **3a–c** have not even arrived at their coalescence points (cf. the SI for plots of the VT spectra).

The structural characterization of a C_1 and a C_2 rotamer was achieved for **3c** and **3a**, respectively (structural details of $\mathbf{3a}^{Ph}$ and $\mathbf{3b}^{Ph}$ in approximate C_2 symmetry are given in the SI). Figure 1 features a juxtaposition of C_1-**3c** (Figure 1a) and C_2-**3a** (Figure 1b). In the first conformer, both bromine atoms are located at the same side of the BC_3 plane; in the second conformer, they are residing at opposite sides of the plane. In a related example, Yamaguchi and co-workers have placed two chlorine atoms in close proximity to a boron center (Figure 1c). They presented evidence for Cl···B interactions and the presence of three-center, four-electron bonds in this pentacoordinated triarylborane.[53] We have selected the following key geometrical parameters to judge whether the structural requirements for similar Br···B interactions are met in C_1-**3c** and C_2-**3a**: (i) the Br···B distances, (ii) the Br···B···Br angles, and (iii) the angles α between the individual Br···B vectors and the respective perpendicular to the BC_3 plane, which has the same spacial orientation as the vacant boron p_z orbital. The sum of the B and Br van der Waals radii (3.75 Å)[54] is significantly larger than any of the Br···B distances found in C_1-**3c** or C_2-**3a** (3.116(2)–3.402(6) Å). However, a closer inspection reveals that C_1-**3c** contains one elongated (3.402(6) Å) together with one shorter distance (3.195(6) Å). The Br···B···Br angles amount to 64.0(1)° in C_1-**3c** and 159.9(4)° in C_2-**3a**. Finally, C_1-**3c** features α values of 29.0° and 43.4°, compared to 20.2° in C_2-**3a**. We further note that the largest α = 43.4° angle is associated with the longest Br···B distance of 3.402(6) Å.

In summary, electron donation from the bromine atoms to the boron centers may indeed contribute to the stabilization of both rotamers, albeit to a different degree, because the C_2 conformation seems to be slightly better suited to accommodate Br···B interactions than the C_1 conformation. Subtle effects of the ethylene or vinylene bridges, which successively contract the C4–C4a–C5 bond angles and thereby pull the bromine donors apart from the boron acceptors, perturb these Br···B interactions so as to render the C_1 rotamer increasingly more competitive. Finally, a mesityl substituent seems to be slightly more compatible with a C_1 conformation, likely on steric grounds. Taking these three competing effects together,

DOI: 10.1021/jacs.7b00268
J. Am. Chem. Soc. 2017, 139, 2842–2851

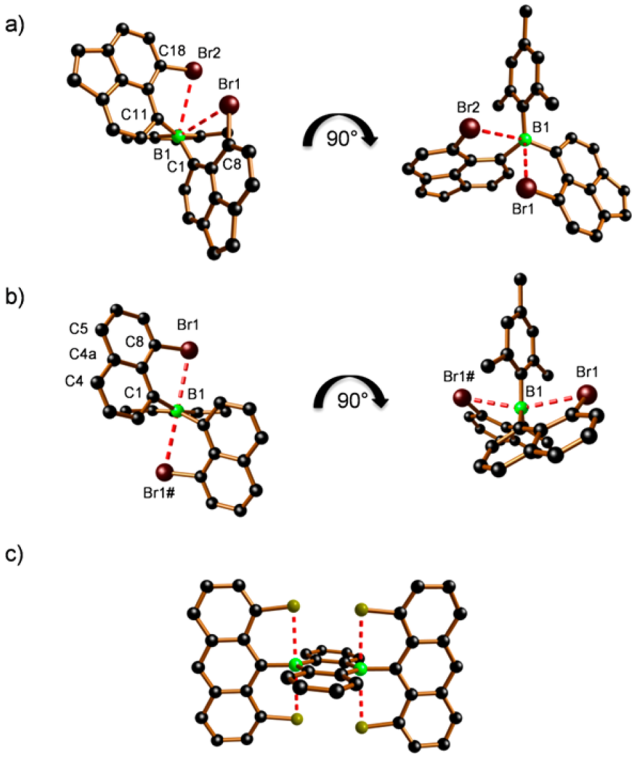

Figure 1. Solid-state structures (H atoms are omitted for clarity): (a) C_1-**3c**, (b) C_2-**3a**, (c) Yamaguchi's pentacoordinated triarylborane[53] with OMes groups omitted.

it becomes reasonable that the C_2 rotamers are more stable in the cases of $\mathbf{3a}^{Ph}$–$\mathbf{3c}^{Ph}$ (no Mes substituents) and **3a** (no peripheral bridge) but that the C_1 rotamers are dominant for **3b** and **3c** (Mes substituents together with peripheral bridges).

As alluded to above, the borepins **4a–c** were deliberately designed to feature a distorted molecular framework in order to guarantee appropriate solubilities, and all three compounds are indeed readily soluble in solvents ranging from alkanes to alcohols. As a downside, crystals suitable for X-ray crystallography are not easily obtained because the compounds tend to form solid foams or resins. Only after numerous efforts did we succeed in growing single crystals of **4a** by slow evaporation of an *n*-hexane/CH_2Cl_2 (1:1) solution (Table 1, top).

For a thorough structural comparison of all three derivatives **4a–c** we additionally relied on quantum-chemical calculations. At the B3LYP/6-31G* level of theory, the twisted borepin scaffolds shown in Table 1 (bottom) represent minima on the potential energy surfaces. All experimentally determined structural parameters of **4a** are in excellent agreement with the corresponding computed values (Table 1).

Expectedly, the mesityl rings of all compounds adopt conformations almost orthogonal to the borepin CBC planes. The B–C bond lengths and C–B–C bond angles of **4a–c** are unexceptional and therefore do not merit further discussion; this is also true for the parent dibenzoborepin **DBB**, the structure of which is included here for comparison (Table 1). **DBB** reveals a slightly bowed geometry in the solid state, which has been attributed to crystal packing effects rather than to a ground-state preference for this particular geometry (dihedral angle between the two annulated benzene rings = 27°).[27] In contrast, **4a–c** possess twisted scaffolds as a result of intramolecular steric repulsion. The twist is most pronounced for **4a** (experimental/computed torsion angle C7–C8–C18–C17 = 39°), whereas **4c** represents the least distorted compound (30°). The same trend has already been deduced from the H7 chemical shift values of **4a–c** (see above) and can be rationalized by the fact that the introduction of ethylene or vinylene linkers into the naphthalene moieties compresses the C4–C4a–C5 bond angles and thereby opens up the bay regions (Table 1); the crystallographically determined C4–C4a–C5 bond angles in the dibromonaphthalene starting materials are 120.4° (**1a**), 111.0(4)° (**1b**), and 109.5(3)° (**1c**).[55–57] Finally, the annulation of two additional benzene rings to the *c* and *e* bonds of **DBB** leads to a significant elongation of the C–C bond opposite to the boron center (marked with *d* in Chart 2), which amounts to 1.342 Å in **DBB**[27] vs 1.502(2) Å in **4a**. Similarly large values have been calculated for the acenaphthene and acenaphthylene derivatives **4b** (1.492 Å) and **4c** (1.487 Å), respectively. These data indicate a localized C=C double-bond in **DBB** but essentially $C(sp^2)$–$C(sp^2)$ single-bond character[58] in the cases of **4a–c**.

C–H Activation in the Course of Yamamoto Coupling. Only the acenaphthene starting material **3b** underwent Ni-mediated dehydrohalogenation (to give **5**) in addition to the Yamamoto dehalogenation coupling reaction (to give **4b**). According to an X-ray crystal-structure analysis of **5**, a bond is again formed between both acenaphthyl substituents (Figure 2; more structural details of **5** are given in the SI). This bond links the formerly brominated carbon atom C8 with C12, which previously carried a hydrogen atom. Importantly, the second bromine atom, which in this case is not required for C–C bond formation, was nevertheless consumed. Compound **5** contains a six-membered BC_5 heterocycle and, apart from the orthogonal mesityl ring, adopts a planar conformation. The serendipitous discovery of this C–H activation reaction provides facile access to the 7-hydro-7-borabenzo[*de*]anthracene class of redox-active luminophores. Previous protocols required multistep synthesis sequences involving a Peterson olefination and a Ru-catalyzed ene–yne cyclization step.[59] Given this background, we did not attempt to only suppress the formation of **5** but rather to develop reaction conditions under which either **4b** or **5** is preferentially generated. To this end, we considered and investigated the

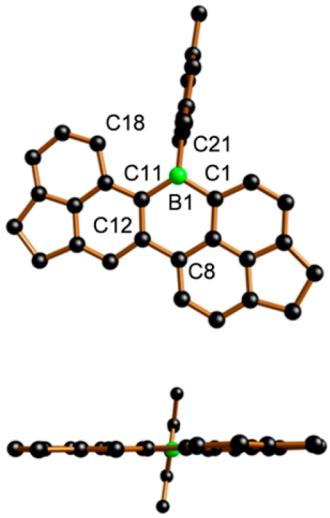

Figure 2. Solid-state structure of **5** (top view and side view; H atoms are omitted for clarity). Selected bond lengths (Å): B1–C1 = 1.555(5), B1–C11 = 1.555(5), B1–C21 = 1.588(4), C8–C12 = 1.481(4).

DOI: 10.1021/jacs.7b00268
J. Am. Chem. Soc. 2017, 139, 2842–2851

following potential influence factors: (i) the reaction temperature and (ii) the local Ni(0) concentration.

The reaction temperature could impact the product distribution because of the rotational barrier about the B−C bonds and/or because Yamamoto-type couplings are normally carried out at elevated temperatures. Several NMR spectroscopic observations argue against a decisive influence of the hindered B−C rotation: (i) Under normal conditions, the naphthalene precursor **3a** prefers a C_2 conformation in solution, whereas for the acenaphthylene precursor **3c** the C_1 rotamer is thermodynamically favored. However, both compounds are almost quantitatively convertible into the corresponding borepins already at room temperature. Thus, either are both conformations suitable for Yamamoto coupling or an equilibrium must exist between both rotamers, which efficiently replenishes the active species on the time scale of the reaction. (ii) Compounds **3a−c** clearly show signs of coalescence in the temperature range 70−80 °C. The rotational barriers should therefore not be unsurmountable at ambient temperature. Indeed, a temperature increase of 30 °C under otherwise identical Yamamoto conditions changes the relative ratio between **4b** and **5** by not more than ±5%.

In order to assess the influence of the local Ni(0) concentration on the **4b**/**5** ratio, we performed the Yamamoto reaction on **3b** at approximately room temperature in three different ways: (A) a solution of the triarylborane was added dropwise to a solution of the preformed, deep purple catalyst system; (B) a solution of **3b**/bpy/COD was treated with neat $Ni(COD)_2$ in one portion; and (C) a dilute solution of the preformed catalyst system was added dropwise to a solution of **3b**. Protocol B represents the standard conditions under which our borepins are usually prepared. The observed ratios **4b**/**5** were approximately 3:1 (protocol A), 1:1 (protocol B), and 1:2.5 (protocol C; Scheme 3). Thus, the local Ni concentration has a decisive influence on the reaction outcome and the borepin **4b** is produced in highest yields when the precursor **3b** is placed in excess Ni(0). As a plausible explanation, the formation of a bond between C8 and C18 requires the insertion of Ni atoms into both C−Br bonds (Figure 1), whereas for the formation of a C8−C12 link only one C−Br bond of **3b** needs to be activated.

We note in passing that this conclusion is also in accordance with our above explanation of why the catalytic borepin formation was not possible.

We next address the question of when the second bromine atom is lost during the assembly of **5**. If the molecule still carried a bromine atom at C18, this substituent would inevitably cause severe steric repulsion of the mesityl group. This unfavorable interaction could facilitate a reaction of the (strained) C−Br bond with Ni(0), and the resulting Ni(II) complex could afterward be quenched by MeOH during workup. Alternatively, loss of a bromine atom after Ni insertion could be a regular background reaction of the Yamamoto coupling of **3b**; both ionic and radical mechanisms are conceivable for this step. The resulting monobrominated triarylborane would only be able to undergo a dehydrohalogenation coupling via C−H activation. Moreover, with this monobrominated starting material, the formation of **5** would no longer be sterically hindered. It is revealing in this context that no brominated **5** was detectable when only 50% of the usual amount of Ni(0) was employed. Under these conditions we rather observed a 50% decrease of the combined yields of **4b** and **5** while the ratio **4b**/**5** remained roughly the same (see the SI for more information).

Up to this point, we have been dealing with the question of which factors are governing the stoichiometric ratio of the C−H activation product **5** and the Yamamoto product **4b**. But there is a second question: Why does the C−H activation reaction occur exclusively with the acenaphthene derivative **3b** and not with the other two triarylboranes? Starting from a precursor molecule in its C_1 conformation, a C−H activation reaction as well as a dehalogenation coupling reaction should be possible. In the C_2 symmetric conformation of any of the three precursor molecules, there are two options to perform a dehydrohalogenation coupling but no obvious one to perform the Yamamoto reaction, because both bromine atoms are located at different sides of the BC_3 plane. Statistically, the transformation leading to compounds of type **5** is therefore more likely to occur than the one leading to borepins, irrespective of the specific precursor employed. Our current working hypothesis regarding the formation of **5** is that a Ni(II) complex, created through the oxidative addition of a C−Br bond, electrophilically attacks the neighboring aromatic substituent at the closest carbon atom C12. Electrophilic attack requires a sufficiently electron-rich π system, a condition that is apparently not met by a naphthyl moiety. The vinylene bridge of acenaphthylene acts as an inductively electron-withdrawing fragment, and this deactivating influence is not overcompensated by an accompanying + M effect because the double bond is essentially localized.[60] The ethylene bridge of acenaphthene, in contrast, exerts a positive inductive effect and therefore facilitates a C−H activation reaction. This line of arguments is further supported by the trend in the HOMO-energy levels of the three arene fragments (B3LYP/6-31G*; cf. Figure S58 in the SI).

A more detailed mechanistic understanding would require extensive quantum-chemical calculations. Unfortunately, even elementary steps of the Yamamoto coupling remain unclear at this time or may differ when different substrates are used: Do the reactions involve mono- or dinuclear Ni complexes? Is the same Ni(0) complex able to perform two successive oxidative addition reactions ultimately furnishing a diaryl Ni(IV) species, or does a substituent redistribution reaction between two monoaryl Ni(II) complexes generate a diaryl Ni(II) intermediate? Are organic radicals[61] and/or Ni(I)/Ni(III) complexes involved?[44,62,63] Given this confusing and sometimes contradicting literature background, we came to the conclusion that DFT calculations are beyond the scope of this publication at the present stage.

Investigations of the Optoelectronic Properties of 4a-c and 5. Cyclic voltammograms of the borepins (THF, 0.1 M $[n\mathrm{Bu_4N}][\mathrm{PF_6}]$, vs $\mathrm{FcH/FcH^+}$) revealed reversible redox events at $E_{1/2}$ = −2.20 (**4a**), −2.38 (**4b**), and −1.49 V (**4c**; Table 2, cf. the SI for CV plots). The acenaphthylene derivative **4c** shows a second reversible redox wave at $E_{1/2}$ = −1.84 V. In the cases of **4a** and **4b**, no further reversible electron transitions are detectable when the sweep is continued into the cathodic regime, but the formerly reversible redox events become irreversible. From these data, the following trend in the LUMO energy levels of **4a−c** can be deduced: **4b** (−2.42 eV) > **4a** (−2.60 eV) > **4c** (−3.31 eV). The same qualitative order was obtained by DFT calculations at the B3LYP/6-31G* level of theory: **4b** (−1.79 eV) > **4a** (−2.03 eV) > **4c** (−2.78 eV; cf. the SI for more details). Even though the absolute energy values show the expected discrepancies between experiment and theory, the energy differences are pleasingly similar. According to the quantum-chemical calculations, **4b** not only possesses the highest lying LUMO but also the highest lying HOMO of

DOI: 10.1021/jacs.7b00268
J. Am. Chem. Soc. 2017, 139, 2842−2851

Table 2. Photophysical and Electrochemical Data of 4a–c, and 5 (Measured in C_6H_{12})

	λ_{abs} (nm) (ε ($M^{-1}cm^{-1}$))	λ_{onset} [a] (nm)	λ_{em} [b] (nm)	ϕ_{PL} [c] (%)	Stokes shift [d] (cm^{-1})	E_{LUMO} [e] (eV)	$E_{1/2}$ [f] (V)	E_{opt} [g] (eV)
4a	408 (12700) 303 (8800)	429	432, 448 [h]	38	1362	−2.60	−2.20	2.89
4b	444 (11800) 321 (7900)	468	462, 488 [h]	52	878	−2.42	−2.38	2.65
4c	444 (10900) 353 (10400)	600				−3.31	−1.49, −1.84	2.07
5	415 (14200) 337 (15200)	450	468, 491 [h]	57	2729	−2.64	−2.16 [i]	2.76
DBB [j]	328 (39800) 260 (122300)	399	400	70		−2.24	−2.56	3.11
DNB(*b,f*) [j]	365 (6800) 314 (15600)	475	477	1		−2.60	−2.20	2.61
DTB [k]	365 (15100) 289 (67600)	378	378	5	942	−2.38	−2.42	3.28

[a]Each onset wavelength was determined by constructing a tangent at the point of infliction of the bathochromic slope of the most red-shifted absorption maximum. [b]λ_{ex} = 400 nm. [c]Absolute quantum yields were determined by using a calibrated integrating sphere. [d]Stokes shifts represent the difference between each longest wavelength absorption maximum and the corresponding shortest wavelength emission maximum. [e]E_{LUMO} = −4.8 eV − $E_{1/2}^{Red1}$ (FcH/FcH^+ = −4.8 eV vs vacuum level). [f]Supporting electrolyte: [nBu$_4$N][PF$_6$] (0.1 M in THF), referenced against the FcH/FcH^+ couple. [g]Excitation energies were calculated from λ_{onset} (E_{opt} = 1240/λ_{onset}). [h]Resolved vibrational finestructure. [i]E_{pc} value of an irreversible reduction process. [j]Reference 27. [k]Reference 33.

the three borepins (−4.99 eV), which is likely attributable to the positive inductive effect of its ethylene bridges. The HOMO of **4c**, on the other hand, is the energetically most favorable one (−5.52 eV). In comparison to **4a**, **DBB** is harder to reduce ($E_{1/2}$ = −2.56 V) while the half-wave potential of **DNB(*b,f*)** is identical to that of **4a** ($E_{1/2}$ = −2.20 V; cf. Chart 2).[27] As a matter of fact, the transition from an annulated benzene ring to a naphthalene moiety considerably facilitates electron injection into the molecule. The specific connectivity, however, between the central borepin ring and the naphthalene fragments seems to be of minor importance, even though it leads to an essentially planar molecular scaffold in **DNB(*b,f*)** vs a heavily twisted scaffold in **4a**. Different from **4a–c**, the electrochemical reduction of PAH **5** is fully irreversible with a cathodic peak potential E_{pc} of −2.16 V.

The longest-wavelength absorption maxima of the pale yellow compound **4a** and the yellow compound **4b** in C_6H_{12} appear at λ_{max} = 408 and 444 nm, respectively (Table 2; Figure 3a,b).

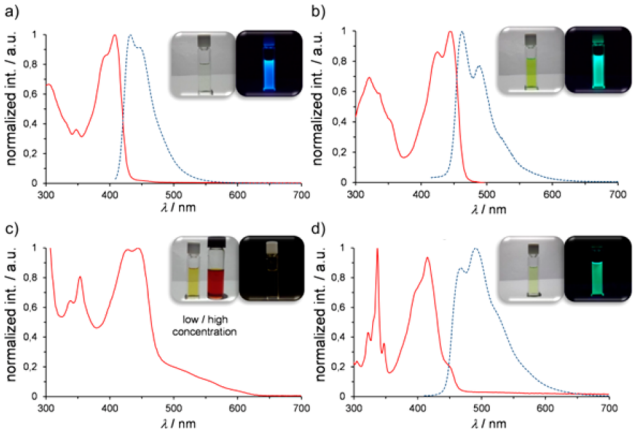

Figure 3. Normalized UV/vis absorption (red) and emission spectra (blue, dotted) of **4a** (a), **4b** (b), **4c** (c), and **5** (d) in C_6H_{12}. Photographs of the compounds in solution under daylight (left) and upon irradiation with a hand-held UV lamp (right, λ_{ex} = 366 nm).

Extremely dilute solutions of the acenaphthylene derivative **4c** appear yellow but adopt a deep red color at higher concentrations. This effect is due to an intense absorption at λ_{max} = 444 nm, accompanied at its bathochromic slope by a very broad and featureless band with an onset at $\lambda_{onset} \approx$ 600 nm (Figure 3c). We tentatively assign this band to a charge-transfer (CT) transition between the HOMO of **4c**, mainly located at the outer rim of the molecule, and the LUMO, which is equally distributed over the entire π-electron system (cf. Figure S58 in the SI). Consistent with its nature as a CT compound, **4c** fluoresces neither in solution nor in the solid state.[64] Contrary to that, solutions of the other two borepins are strongly emissive upon photoexcitation. Starting from **DBB** (λ_{em} = 400 nm; fluorescence quantum yield ϕ_{PL} = 70%)[27] annulation of two more benzene rings to give **4a** results in a moderate red-shift of the emission maximum (λ_{em} = 432 nm) and a 50% decrease in ϕ_{PL} to a value of 38%. Linear annulation to give **DNB(*b,f*)** leads to a more pronounced bathochromic shift (λ_{em} = 477 nm) and a drastic drop in ϕ_{PL} to only 1%.[27] When two ethylene bridges are introduced at the periphery of **4a**, the resulting **4b** (λ_{em} = 462 nm) fluoresces at a similar wavelength as **DNB(*b,f*)** but the quantum efficiency remains at a high level of ϕ_{PL} = 52%. The C–H-activation product **5** absorbs at λ_{max} = 415 nm, emits at λ_{em} = 468 nm, and thus shows the largest Stokes shift of all four species ($\Delta\bar{\nu}$ = 2729 cm^{-1}; Figure 3d). Not only λ_{em} but also the quantum yield (ϕ_{PL} = 57%) are similar to those of the corresponding borepin **4b**.

III. CONCLUSION

Herein we disclose a convenient, modular, and high-yielding approach for the preparation of annulated borepins. Their potential applications range from Lewis acid catalysts to optoelectronic materials. Starting from stable, ubiquitous aryl–BF_3K salts, we first introduce two (substituted) 8-bromonaphthyl moieties ($Naph^{Br,R}$) to obtain heteroleptic triarylboranes of the form aryl–B($Naph^{Br,R}$)$_2$ (aryl = mesityl, phenyl). In the key step of the synthesis sequence, closure of the seven-membered ring is achieved through an intramolecular Ni-mediated Yamamoto dehalogenation coupling reaction. All presented borepins are quadruply benzannulated. The distribution of the benzene rings around the heterocyclic core was deliberately designed to form a distorted bay region and consequently to improve the solubility of the compounds, even in the absence of solubilizing side chains. As a further advantage, our mesityl-substituted borepins were found to be fully inert toward air and moisture, which distinguishes them from almost all other known borepins that need to be protected by sterically more demanding supermesityl groups (Mes* = 2,4,6-tri-*tert*-butylpenyl). Most notably, we found a strong influence of peripheral and seemingly innocent substituents R on the reactivity and the optoelectronic properties of the quadruply benzannulated borepins: (i) The coupling of triarylboranes Mes–B($Naph^{Br,R}$)$_2$ with $HNaph^{Br,R}$ = 8-bromonaphthalene (no further substituent) or 5-bromoacenaphthylene (vinylene bridge) furnishes the

DOI: 10.1021/jacs.7b00268
J. Am. Chem. Soc. 2017, 139, 2842–2851

corresponding borepins, **4a** and **4c**, in close to quantitative yields. When the same reaction conditions are applied to Mes−B(Naph^{Br,R})$_2$ with HNaph^{Br,R} = 5-bromoacenaphthene (ethylene bridge), dehalogenative coupling to afford the borepin **4b** is invariably accompanied by a dehydrohalogenative coupling reaction to give the annulated six-membered boron heterocycle **5**. The product ratio **4b**/**5** is mainly governed by the local Ni(0) concentration and can thus be varied between 3:1 (high concentration) and 1:2.5 (low concentration). (ii) The redox potential of **4c** (−1.49 V) is less cathodic by 0.71 or 0.89 V compared to that of **4a** or **4b**, respectively. (iii) Borepin **4a** is photoluminescent in the blue region of the spectrum (λ_{em} = 432 nm, ϕ_{PL} = 38%). The introduction of ethylene bridges into the naphthyl fragments shifts the emission wavelength of **4b** bathochromically by 30 nm and improves the quantum efficiency by 14% (λ_{em} = 462 nm, ϕ_{PL} = 52%). In stark contrast, **4c**, which carries two vinylene bridges, is nonfluorescent.

■ ASSOCIATED CONTENT

Supporting Information

The Supporting Information is available free of charge on the ACS Publications website at DOI: 10.1021/jacs.7b00268.

Experimental details and NMR data of **3a**−**c**, **3a**^{Ph}−**3c**^{Ph}, **4a**−**c** and **5**; X-ray crystal structure analyses of **3a**, **3c**, **3a**^{Ph}, **3b**^{Ph}, **4a**, and **5**; mass spectrometric characterization of **4a**−**c** and **5**; cyclic voltammograms of compounds **4a**−**c** and **5**; absorption and emission spectra of the compounds **4a**−**c** and **5** in C_6H_{12}; variable-temperature ^{1}H NMR spectra of **3a**−**c** and **3b**^{Ph}−**3c**^{Ph} in toluene-d_8; computational details for compounds **4a**−**c** and **5** (PDF)

X-ray crystal structure analyses of **3a**, **3c**, **3a**^{Ph}, **3b**^{Ph}, **4a**, and **5** (CIF)

Optimized structures of **4a**−**c** and **5** (XYZ)

■ AUTHOR INFORMATION

Corresponding Author

*matthias.wagner@chemie.uni-frankfurt.de

ORCID

Matthias Wagner: 0000-0001-5806-8276

Notes

The authors declare no competing financial interest.

■ ACKNOWLEDGMENTS

Donations of lithium organyls by Albemarle Lithium GmbH are gratefully acknowledged.

■ REFERENCES

(1) Jäkle, F. *Chem. Rev.* **2010**, *110*, 3985−4022.

(2) Lorbach, A.; Hübner, A.; Wagner, M. *Dalton Trans.* **2012**, *41*, 6048−6063.

(3) Rao, Y.-L.; Amarne, H.; Wang, S. *Coord. Chem. Rev.* **2012**, *256*, 759−770.

(4) Narita, A.; Wang, X.-Y.; Feng, X.; Müllen, K. *Chem. Soc. Rev.* **2015**, *44*, 6616−6643.

(5) Ren, Y.; Jäkle, F. *Dalton Trans.* **2016**, *45*, 13996−14007.

(6) (a) Zhang, Z.; Edkins, R. M.; Haehnel, M.; Wehner, M.; Eichhorn, A.; Mailänder, L.; Meier, M.; Brand, J.; Brede, F.; Müller-Buschbaum, K.; Braunschweig, H.; Marder, T. B. *Chem. Sci.* **2015**, *6*, 5922−5927. (b) Braunschweig, H.; Fernandez, I.; Frenking, G.; Kupfer, T. *Angew. Chem., Int. Ed.* **2008**, *47*, 1951−1954. (c) Fan, C.; Piers, W. E.; Parvez, M. *Angew. Chem., Int. Ed.* **2009**, *48*, 2955−2958. (d) Jimenez-Halla, J. O.; Matito, E.; Sola, M.; Braunschweig, H.; Horl, C.; Krummenacher, I.; Wahler, J. *Dalton Trans.* **2015**, *44*, 6740−6747. (e) Yruegas, S.; Martin, C. D. *Chem. - Eur. J.* **2016**, *22*, 18358−18361. (f) Barnard, J. H.; Yruegas, S.; Huang, K.; Martin, C. D. *Chem. Commun.* **2016**, *52*, 9985−9991. (g) Yruegas, S.; Huang, K.; Wilson, D. J. D.; Dutton, J. L.; Martin, C. D. *Dalton Trans.* **2016**, *45*, 9902−9911. Review articles: (h) Escande, A.; Ingleson, M. J. *Chem. Commun.* **2015**, *51*, 6257−6274. (i) Ji, L.; Griesbeck, S.; Marder, T. B. *Chem. Sci.* **2017**, *8*, 846−863. (j) Steffen, A.; Ward, R. M.; Jones, W. D.; Marder, T. B. *Coord. Chem. Rev.* **2010**, *254*, 1950−1976. (k) Braunschweig, H.; Kupfer, T. *Chem. Commun.* **2011**, *47*, 10903−10914.

(7) Messersmith, R. E.; Tovar, J. D. *J. Phys. Org. Chem.* **2015**, *28*, 378−387.

(8) Iida, A.; Sekioka, A.; Yamaguchi, S. *Chem. Sci.* **2012**, *3*, 1461−1466.

(9) Ashe, A. J.; Kampf, J. W.; Nakadaira, Y.; Pace, J. M. *Angew. Chem., Int. Ed. Engl.* **1992**, *31*, 1255−1258.

(10) Ashe, A. J.; Klein, W.; Rousseau, R. *Organometallics* **1993**, *12*, 3225−3231.

(11) Pasinski, J. P. *J. Chem. Phys.* **1974**, *61*, 683−691.

(12) Budzelaar, P. H. M.; van der Kerk, S. M.; Krogh-Jespersen, K.; Schleyer, P. v. R. *J. Am. Chem. Soc.* **1986**, *108*, 3960−3967.

(13) Onak, T.; Diaz, M.; Barfield, M. *J. Am. Chem. Soc.* **1995**, *117*, 1403−1410.

(14) Lu, Z.; Schweighauser, L.; Hausmann, H.; Wegner, H. A. *Angew. Chem., Int. Ed.* **2015**, *54*, 15556−15559.

(15) Schweighauser, L.; Wegner, H. A. *Chem. - Eur. J.* **2016**, *22*, 14094−14103.

(16) von Grotthuss, E.; Diefenbach, M.; Bolte, M.; Lerner, H.-W.; Holthausen, M. C.; Wagner, M. *Angew. Chem., Int. Ed.* **2016**, *55*, 14067−14071.

(17) (a) Numata, M.; Yasuda, T.; Adachi, C. *Chem. Commun.* **2015**, *51*, 9443−9446. (b) Li, D.; Zhang, H.; Wang, Y. *Chem. Soc. Rev.* **2013**, *42*, 8416−8433.

(18) For further information, see also ref 6h,i.

(19) Hübner, A.; Qu, Z. W.; Englert, U.; Bolte, M.; Lerner, H.-W.; Holthausen, M. C.; Wagner, M. *J. Am. Chem. Soc.* **2011**, *133*, 4596−4609.

(20) Hübner, A.; Diefenbach, M.; Bolte, M.; Lerner, H.-W.; Holthausen, M. C.; Wagner, M. *Angew. Chem., Int. Ed.* **2012**, *51*, 12514−12518.

(21) Lorbach, A.; Bolte, M.; Li, H.; Lerner, H.-W.; Holthausen, M. C.; Jäkle, F.; Wagner, M. *Angew. Chem., Int. Ed.* **2009**, *48*, 4584−4588.

(22) Lorbach, A.; Bolte, M.; Lerner, H.-W.; Wagner, M. *Chem. Commun.* **2010**, *46*, 3592−3594.

(23) Hübner, A.; Diehl, A. M.; Bolte, M.; Lerner, H.-W.; Wagner, M. *Organometallics* **2013**, *32*, 6827−6833.

(24) Hübner, A.; Diehl, A. M.; Diefenbach, M.; Endeward, B.; Bolte, M.; Lerner, H.-W.; Holthausen, M. C.; Wagner, M. *Angew. Chem., Int. Ed.* **2014**, *53*, 4832−4835.

(25) Kaese, T.; Hübner, A.; Bolte, M.; Lerner, H.-W.; Wagner, M. *J. Am. Chem. Soc.* **2016**, *138*, 6224−6233.

(26) For applications of 9,10-diaryl-9,10-dihydro-9,10-diboraanthracenes as redox-active, photoluminescent compounds, see: (a) Januszewski, E.; Bolte, M.; Lerner, H.-W.; Wagner, M. *Organometallics* **2012**, *31*, 8420−8425. (b) Hoffend, C.; Schödel, F.; Bolte, M.; Lerner, H.-W.; Wagner, M. *Chem. - Eur. J.* **2012**, *18*, 15394−15405. (c) Hoffend, C.; Diefenbach, M.; Januszewski, E.; Bolte, M.; Lerner, H.-W.; Holthausen, M. C.; Wagner, M. *Dalton Trans.* **2013**, *42*, 13826−13837. (d) Reus, C.; Weidlich, S.; Bolte, M.; Lerner, H.-W.; Wagner, M. *J. Am. Chem. Soc.* **2013**, *135*, 12892−12907. (e) Hoffend, C.; Schickedanz, K.; Bolte, M.; Lerner, H.-W.; Wagner, M. *Tetrahedron* **2013**, *69*, 7073−7081. (f) Reus, C.; Guo, F.; John, A.; Winhold, M.; Lerner, H.-W.; Jäkle, F.; Wagner, M. *Macromolecules* **2014**, *47*, 3727−3735.

(27) Mercier, L. G.; Piers, W. E.; Parvez, M. *Angew. Chem., Int. Ed.* **2009**, *48*, 6108−6111.

(28) Mercier, L. G.; Furukawa, S.; Piers, W. E.; Wakamiya, A.; Yamaguchi, S.; Parvez, M.; Harrington, R. W.; Clegg, W. *Organometallics* **2011**, *30*, 1719−1729.

DOI: 10.1021/jacs.7b00268
J. Am. Chem. Soc. 2017, 139, 2842−2851

(29) Caruso, A., Jr.; Siegler, M. A.; Tovar, J. D. *Angew. Chem., Int. Ed.* **2010**, *49*, 4213−4217.
(30) Caruso, A., Jr.; Tovar, J. D. *J. Org. Chem.* **2011**, *76*, 2227−2239.
(31) Caruso, A., Jr.; Tovar, J. D. *Org. Lett.* **2011**, *13*, 3106−3109.
(32) Levine, D. R.; Caruso, A., Jr.; Siegler, M. A.; Tovar, J. D. *Chem. Commun.* **2012**, *48*, 6256−6258.
(33) Levine, D. R.; Siegler, M. A.; Tovar, J. D. *J. Am. Chem. Soc.* **2014**, *136*, 7132−7139.
(34) Messersmith, R. E.; Siegler, M. A.; Tovar, J. D. *J. Org. Chem.* **2016**, *81*, 5595−5605.
(35) Schickedanz, K.; Trageser, T.; Bolte, M.; Lerner, H.-W.; Wagner, M. *Chem. Commun.* **2015**, *51*, 15808−15810.
(36) The serendipitous formation of a borylated **DBB** through skeletal rearrangement has also been reported. Iida, A.; Saito, S.; Sasamori, T.; Yamaguchi, S. *Angew. Chem., Int. Ed.* **2013**, *52*, 3760−3764.
(37) (a) Churches, Q. I.; Hooper, J. F.; Hutton, C. A. *J. Org. Chem.* **2015**, *80*, 5428−5435. (b) Frohn, H.-J.; Franke, H.; Fritzen, P. *J. Organomet. Chem.* **2000**, *598*, 127−135.
(38) (a) Darses, S.; Genet, J. P. *Eur. J. Org. Chem.* **2003**, *2003*, 4313−4327. (b) Molander, G. A.; Ellis, N. *Acc. Chem. Res.* **2007**, *40*, 275−286. (c) Darses, S.; Genet, J. P. *Chem. Rev.* **2008**, *108*, 288−325. (d) Molander, G. A. *J. Org. Chem.* **2015**, *80*, 7837−7848.
(39) We usually add Me_3SiCl at the beginning of the workup process to ensure that residual fluoride ions are removed. The presence of Me_3SiCl is not a prerequisite for the formation of **3a**−**c**. If the introduction of the naphthyl substituents proceeds via a Mes−BF_2 intermediate, the Li^+ ion would then have to take the role of the fluoride-abstracting reagent.
(40) Samigullin, K.; Bolte, M.; Lerner, H.-W.; Wagner, M. *Organometallics* **2014**, *33*, 3564−3569.
(41) A first example of a 2-fold substitution reaction of lithiated intermediates on aryl trifluoroborates is given in ref 6a.
(42) Gyömöre, Á.; Bakos, M.; Földes, T.; Pápai, I.; Domján, A.; Soós, T. *ACS Catal.* **2015**, *5*, 5366−5372.
(43) Samigullin, K.; Soltani, Y.; Lerner, H.-W.; Wagner, M.; Bolte, M. *Acta Crystallogr., Sect. C: Struct. Chem.* **2016**, *72*, 189−197.
(44) Rosen, B. M.; Quasdorf, K. W.; Wilson, D. A.; Zhang, N.; Resmerita, A. M.; Garg, N. K.; Percec, V. *Chem. Rev.* **2011**, *111*, 1346−1416.
(45) Iyoda, M.; Sato, K.; Oda, M. *Tetrahedron Lett.* **1985**, *26*, 3829−3832.
(46) Colon, I.; Kelsey, D. R. *J. Org. Chem.* **1986**, *51*, 2627−2637.
(47) Percec, V.; Bae, J.-Y.; Zhao, M.; Hill, D. H. *J. Org. Chem.* **1995**, *60*, 176−185.
(48) Yamamoto, T.; Wakabayashi, S.; Osakada, K. *J. Organomet. Chem.* **1992**, *428*, 223−237.
(49) It is generally agreed upon that aryl bromides tend to react significantly slower than aryl chlorides under the conditions of a catalytic Colon reaction. In our hands, the conversion of chlorobenzene to biphenyl also proceeded significantly faster than the coupling of bromobenzene; see refs 46 and 47.
(50) Nöth, H.; Wrackmeyer, B. *Nuclear Magnetic Resonance Spectroscopy of Boron Compounds*. In *NMR Basic Principles and Progress*; Diehl, P., Fluck, E., Kosfeld, R., Eds.; Springer: Berlin, 1978.
(51) Matsuo, K.; Saito, S.; Yamaguchi, S. *J. Am. Chem. Soc.* **2014**, *136*, 12580−12583.
(52) Hertz, V. M.; Bolte, M.; Lerner, H.-W.; Wagner, M. *Angew. Chem., Int. Ed.* **2015**, *54*, 8800−8804.
(53) Dou, C.; Saito, S.; Yamaguchi, S. *J. Am. Chem. Soc.* **2013**, *135*, 9346−9349.
(54) Mantina, M.; Chamberlin, A. C.; Valero, R.; Cramer, C. J.; Truhlar, D. G. *J. Phys. Chem. A* **2009**, *113*, 5806−5812.
(55) Haltiwanger, R. C.; Beurskens, P. T.; Vankan, J. M. J.; Veeman, W. S. *J. Crystallogr. Spectrosc. Res.* **1984**, *14*, 589−597.
(56) Aschenbach, L. K.; Knight, F. R.; Randall, R. A.; Cordes, D. B.; Baggott, A.; Buhl, M.; Slawin, A. M.; Woollins, J. D. *Dalton Trans.* **2012**, *41*, 3141−3153.
(57) Diamond, L. M.; Knight, F. R.; Athukorala Arachchige, K. S.; Randall, R. A. M.; Bühl, M.; Slawin, A. M. Z.; Woollins, J. D. *Eur. J. Inorg. Chem.* **2014**, *2014*, 1512−1523.
(58) Whitesell, J. K.; Fox, M. A. *Organic Chemistry*, 3rd ed.; Jones & Bartlett: Boston, 2004; p 77.
(59) Hertz, V. M.; Lerner, H.-W.; Wagner, M. *Org. Lett.* **2015**, *17*, 5240−5243.
(60) Neilson, A. N. *PAHs and related compounds: Chemistry*, 1st ed.; Springer-Verlag: Berlin, 2013; Vol. 3.
(61) A related C−Br/C−H coupling reaction involving radical intermediates has previously been carried out on tris(8-bromonaphth-1-yl)borane using $(Me_3Si)_3SiH$ and 1,1′-azobis(cyclohexanecarbonitrile); see ref 51.
(62) Tsou, T. T.; Kochi, J. K. *J. Am. Chem. Soc.* **1979**, *101*, 7547−7560.
(63) Matsubara, K.; Yamamoto, H.; Miyazaki, S.; Inatomi, T.; Nonaka, K.; Koga, Y.; Yamada, Y.; Veiros, L. F.; Kirchner, K. *Organometallics* **2017**, *36*, 255−265.
(64) Note that acenaphthylene itself is a nonfluorescent compound: Plummer, B. F.; Hopkinson, M. J.; Zoeller, J. H. *J. Am. Chem. Soc.* **1979**, *101*, 6779−6781.

DOI: 10.1021/jacs.7b00268
J. Am. Chem. Soc. 2017, 139, 2842−2851